Two Methanes are Better than One: A Density Functional Theory Study of the Reactions of $Mo_2O_y^-$ ($y = 2-5$) with Methane

Nicholas J. Mayhall and Krishnan Raghavachari*

Department of Chemistry, Indiana University, Bloomington, Indiana 47405

Received: June 22, 2007

The mechanisms of chemical reactions of molybdenum suboxide clusters $Mo_2O_n^-$ ($n = 2-5$) with methane are investigated using B3LYP hybrid density functional theory and polarized basis sets. In particular, we focus on the reactions of the most stable structural isomers of $Mo_2O_{2,3,4,5}^-$ that lead to single molybdenum species such as $HMoO_2CH_3^-$, as seen in the recent experimental study of Jarrold and co-workers. We find that, while all experimentally observed products are unfavorable due to the high amount of energy required to cleave the metal oxide, the formation of $HMoO_2CH_3^-$ is least endothermic. Even in this case, the thermodynamics of these reactions is very unfavorable when a *single methane* is reacted with the metal oxide. However, we find that the sequential addition of *two methanes* produces $HMoO_2CH_3^-$ (and another neutral molecule whose identity depends on the number of oxygens in the metal oxide) at a much lower thermodynamic cost. Further, *the overall reaction barriers are much lower when the second methane adds prior to the* $Mo_2O_{2,3,4,5}^-$ *cleavage*. The methane addition at each metal center oxidizes the metals to produce a species that is then stable enough to afford the Mo−Mo cleavage.

I. Introduction

New developments in catalytic activation of methane, such as the dehydrogenation−aromatization of methane (DHAM),[1−6] have motivated studies on reactions between methane and transition metal oxides.[7,8] In recent years, transition metal oxides have proven to be very effective in the catalysis of many C−H bond activating reactions.[9−16] These reactions have stimulated substantial interest due to the utility of C−H bond cleavage and the difficulty normally associated with achieving it in practice. Transition metal oxides, in particular group VIB metal oxides, have received significant attention in the literature due to their electronic and structural properties.[17−24]

Recently, molybdenum suboxide cluster anions ($Mo_xO_y^-$, where $y/x < 3$) have been the focus of reactivity studies with methane and ethane. By analyzing the mass spectra of the products formed in such reactions, Jarrold and co-workers[7] have identified several individual molecular species. In particular, for the reactions of methane with clusters consisting mostly of MoO_y^- and $Mo_2O_y^-$, the dominant new product masses correspond to the molecular formulas $MoCH_2^-$, $MoOCH_2^-$, and $MoO_2CH_4^-$. Through mass specific anion photoelectron spectra coupled with DFT calculations, they have also assigned the possible isomeric structures of the products formed. In particular, the $HMoO_2CH_3^-$ isomeric structure containing a central Mo coordinated to two oxygens, a hydrogen, and a methyl group (stoichiometry $MoO_2CH_4^-$) was found to be the most energetically favorable product.

The appearance of these products is evidence of novel methane−molybdenum suboxide chemistry. By increasing the relative concentration of methane in the experiment, Wyrwas et al.[7] have found that the $Mo_2O_y^-$ manifold decreases while the MoO_y^- manifold increases. This suggests that, upon reaction with methane, clusters containing two molybdenum centers are undergoing a cleavage to yield two single molybdenum species. It should be mentioned that, as shown previously by Xu et al.[8] and Wyrwas et al.,[7] the single molybdenum cluster, MoO_2^-, reacts exothermically with methane to produce $HMoO_2CH_3^-$. However, it is quite unlikely that MoO_2^- alone is responsible for the entire formation of $HMoO_2CH_3^-$ because the experimental abundance of MoO_2^- is very low. In addition, it would not explain the decreasing $Mo_2O_y^-$ concentration with increasing methane concentration. Therefore, this study focuses on the reactive interactions between clusters with two molybdenums and methane.

Among the product ions observed experimentally, preliminary calculations have shown $HMoO_2CH_3^-$ to be the most thermodynamically accessible product. This is not surprising because the formal oxidation state of Mo in the corresponding neutral compound is +6, the value found in stable Mo compounds such as MoO_3. The formation of $HMoO_2CH_3^-$ suggests a classic oxidative addition reaction where a metal center in a lower oxidation state inserts into methane's C−H bond. Although the masses of the products have been measured experimentally and the geometries have been optimized computationally,[7] a mechanistic explanation of the appearance of these peaks has yet to be proposed. In particular, the experimental reactivity studies have not yet been performed with individual mass selected clusters. Difficulties in mapping complete reaction paths arise due to the simultaneous presence of each reactant ion in the initial cluster beam. Because all metal oxides are created at the same time, the correspondence between specific reactants and specific products is not obvious. Through the theoretical investigation of these reactions, we seek to develop a better understanding of the reactive interactions between hydrocarbons and metal oxides.

The computational study presented has a threefold purpose. We aim (i) to determine which reactants are most likely responsible for the experimentally observed products, (ii) to give a mechanistic account of the experimentally observed reactions

* Corresponding author. Email:kraghava@indiana.edu.

10.1021/jp074894m CCC: $37.00
Published on Web 08/01/2007

TABLE 1: Basis Set Effects on the Computed Reaction Energies

ΔE	SDDplus	triple ζ
$Mo_2O_2^-$	9.62	9.66
$Mo_2O_3^-$	13.04	14.16
$Mo_2O_4^-$	21.15	20.75

between molybdenum suboxides and methane, with a focus on $HMoO_2CH_3^-$ as the most favorable product, and (iii) to generalize the experimental observations to better understand molybdenum oxide chemistry.

II. Computational Details

All calculations reported (except where otherwise noted) have been performed using the B3LYP hybrid density functional method, which contains a parametrized combination of Hartree−Fock exchange, Becke's gradient corrected exchange functional and the Lee−Yang−Parr exchange-correlation functional.[25,26] We have replaced the 28 core electrons of molybdenum with the Stuttgart−Dresden (SDD) relativistic pseudopotential, using an augmented version of the associated double-ζ basis set to describe the remaining 14 valence electrons.[27−29] For the remaining atoms (H, C, and O), we start with the double-ζ D95 sp basis set.[31] To properly describe the anion's extended radial wave function, diffuse functions were added to all atomic centers (s, p, and d functions on Mo; s and p functions on C and O, s functions on H) using an exponent ratio of 0.3 to maintain even-tempered basis set behavior.[30] To allow for greater angular flexibility in optimizing the molecular orbitals, a single polarization function of $l + 1$ angular momentum was added to each atomic center ($\zeta = 0.3$ for *f* on Mo, $\zeta = 1.292$ for *d* on O, $\zeta = 0.626$ for *d* on C, and $\zeta = 0.75$ for *p* on H). The diffuse and polarization functions, whose exponents can be found in the Supporting Information, result in the augmented basis set that has been denoted as "SDDplus".

Basis set convergence was investigated by a series of calculations using the B3LYP functional along with augmented triple-ζ quality basis sets. For Mo, the Stuttgart relativistic pseudopotentials and basis sets, augmented with two *f*-type functions and one *g*-type function were used, following the recommendations by Martin and Sundermann.[32] For all other atoms, the aug-cc-pVTZ basis sets[33] were used. The basis set dependencies in our calculated results are quite minimal and are displayed in Table 1.

All calculations were performed using the development version of the Gaussian suite of electronic structure programs.[34] Vibrational frequency analysis of each stationary point was performed to ensure that the optimized geometry is a true minimum or a first-order saddle point in the case of transition states. For each calculated reaction barrier, an intrinsic reaction coordinate (IRC) calculation was performed to ensure that the optimized transition state truly connects the reactants and products. Because of the high spin state of the Mo atom (septet), predicting the most favorable electronic state for the suboxide systems is not trivial. For each structure presented, all plausible spin states were explored systematically. The reported reaction profiles display the energy of the lowest spin state for each point along the curve. In some cases, we observed the multiplicity changing during the course of the reaction. This is to be expected because the reaction with methane saturates the reactive (high spin) metal oxides, making the lower spin potential energy surface to become more stable than the higher spin potential energy surface. However, to maintain the flow of the discussion, we have shown the reaction profiles as simple smoothly connected curves.

III. Results and Discussion

A. $Mo_2O_y^- + CH_4$. The thermodynamics of the reactions between the lowest energy isomer of each molybdenum oxide cluster anion and methane have been illustrated in Table 2 below. It should be noted that in all but one case $HMoO_2CH_3^-$ is the most thermodynamically accessible product formed from a particular molybdenum oxide. This is due to the fact that, as already mentioned, $HMoO_2CH_3^-$ is sufficiently saturated with oxidizing bonds. The one exception is in the set of reactions in Table 2 between $Mo_2O_4^-$ and methane, where the last reaction is the least endothermic. This is a consequence of MoO_2 having a higher electron affinity than $HMoO_2CH_3$.

In efforts to find the lowest energy reaction channel for the production of $HMoO_2CH_3^-$, and hence the most probable mechanism, an exhaustive transition state search was performed for each of the lowest energy structural isomers of $Mo_2O_y^-$ ($y = 2-5$) with methane. To facilitate the following discussion, we use a previously introduced notation for distinguishing between structural isomers of the $Mo_2O_y^-$ series. The isomers are denoted by the number "ABC", where A and C represent the number of peripheral oxygens attached to the two molybdenum atoms and B denotes the number of bridging oxygens.

As seen from the results above, the reaction between $Mo_2O_2^-$ and methane is the most thermodynamically favorable option for production of $HMoO_2CH_3^-$. The reactions of the "200" isomer of $Mo_2O_2^-$, previously shown to be the lowest energy form, with a single methane are shown in Figure 1.[35] It is clear that the lowest energy transition state does not lead to the products $HMoO_2CH_3^-$ and Mo. To produce $HMoO_2CH_3^-$ from $Mo_2O_2^-$ and methane, higher energy transition states must be visited.

Figure 2 shows $Mo_2O_2^-$ reacting with methane to form $HMoO_2CH_3^-$ and Mo through a mechanism (denoted $C^{\ddagger}$) that is not the lowest energy pathway. Because $Mo_2O_2^-$, in order to produce the experimentally observed products, must form this higher energy transition state, the reaction has a very large barrier of 40.2 kcal/mol. It is assumed that the experimental set up is sufficiently cool such that the formation of the dissociation product from these mechanisms is unlikely.

Figures 3 and 4 show the reactions of the "111" and "210" isomers of $Mo_2O_3^-$ with methane. Though they represent the most thermodynamically favorable reactions, they are still very endothermic, with energies of reaction higher than 40 kcal/mol. Figures 5 and 6 show a single methane reacting with the two lowest energy isomers of $Mo_2O_4^-$. Although the energy barriers for the initial insertion of methane are quite low (10.7 and 5.9 kcal/mol for 121 and 211, respectively), both overall reactions are endothermic by more than 55 kcal/mol. $Mo_2O_5^-$ reactions are not shown here because they are endothermic by about 80 kcal/mol and not likely to occur.

Thus, all of the reactions between a single methane and $Mo_2O_y^-$ ($y = 2, 5$) either are too endothermic or have reaction barriers that are too high to be possible mechanisms for the experimentally observed reactions. Thus the simple reaction scheme of a single methane oxidatively adding to the molybdenum center is inadequate to describe the products seen experimentally. More complex reactions must be investigated. Because experimentally the concentration of methane is much greater than that of the metal species, it is reasonable to expect a second reaction with methane. This would increase the oxidation of the second molybdenum, thus stabilizing the neutral product.

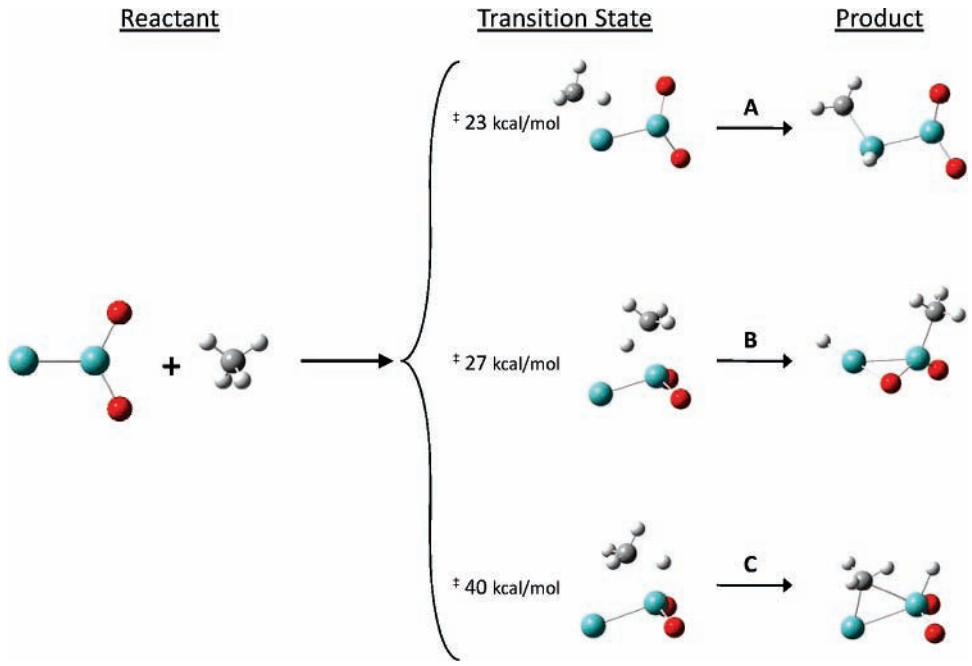

Figure 1. Reaction schemes for the reaction of the 200 isomer of $Mo_2O_2^-$ with methane.

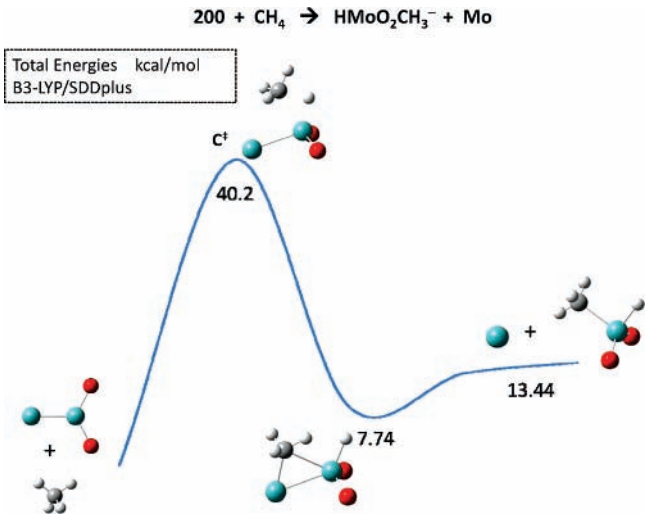

Figure 2. Reaction energy profile for the reaction of the 200 isomer of $Mo_2O_2^-$ with methane.

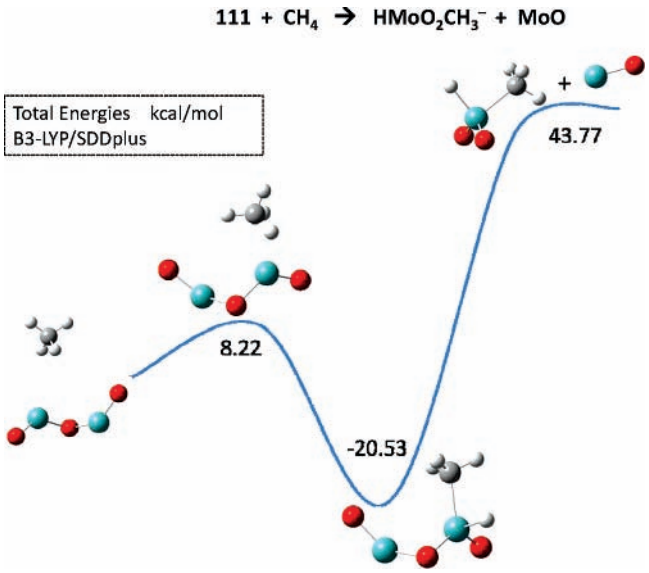

Figure 3. Reaction energy profile for the reaction of the 111 isomer of $Mo_2O_3^-$ with methane.

B. $Mo_2O_y^- + 2CH_4$. Table 3 summarizes reactions between the lowest structural isomer of each molybdenum oxide with two methanes that lead to the formation of *the same ionic product*. The key point to note is that, by adding a second methane, the neutral product has been stabilized, thus lowering the total reaction endothermicity. Because the experimental data contains only information about charged species, the neutral product is able to be manipulated without affecting the comparison to experiment. The energies in Table 3 reflect the increasing stability of the $Mo_xO_y^-$ species as $y/x \rightarrow 3$ (stability: $Mo_2O_2^- < Mo_2O_3^- < Mo_2O_4^- < Mo_2O_5^-$).

There are two types of mechanisms one could anticipate for the reactions listed in Table 3.

(1) The $Mo_2O_y^-$ could insert itself into the C−H bond and then fragment as in Figures 2−6. The resulting neutral product could then insert itself into the C−H bond of another methane

TABLE 2: B3LYP/SDDplus Reaction Energies and Zero-Point Corrected Energies, in kcal/mol, of Reactions of $Mo_2O_n^-$, with Methane Producing Desired Products

			ΔE	ΔE + zpe				ΔE	ΔE + zpe
$Mo_2O_2^- + CH_4$	→	$MoCH_2^- + H_2MoO_2$	71.7	64.8	$Mo_2O_3^- + CH_4$	→	$MoCH_2^- + H_2MoO_3$	79.1	75.4
		$MoOCH_2^- + HMoOH$	72.1	66.8			$MoOCH_2^- + H_2MoO_2$	63.5	57.9
		$HMoO_2CH_3^- + Mo$	13.4	11.1			$HMoO_2CH_3^- + MoO$	43.8	40.9
		$MoO_2^- + HMoCH_3$	42.6	38.6			$MoO_2^- + HMoOCH_3$	46.0	42.2
$Mo_2O_4^- + CH_4$	→	$MoCH_2^- + H_2MoO_4$	103.9	101.8	$Mo_2O_5^- + CH_4$	→	$MoCH_2^- + H_2MoO_5$		
		$MoOCH_2^- + H_2MoO_3$	80.3	76.5			$MoOCH_2^- + H_2MoO_4$	102.2	100.6
		$HMoO_2CH_3^- + MoO_2$	57.2	53.9			$HMoO_2CH_3^- + MoO_3$	81.6	79.0
		$MoO_2^- + HMoO_2CH_3$	54.2	51.7			$MoO_2^- + HMoO_3CH_3$		

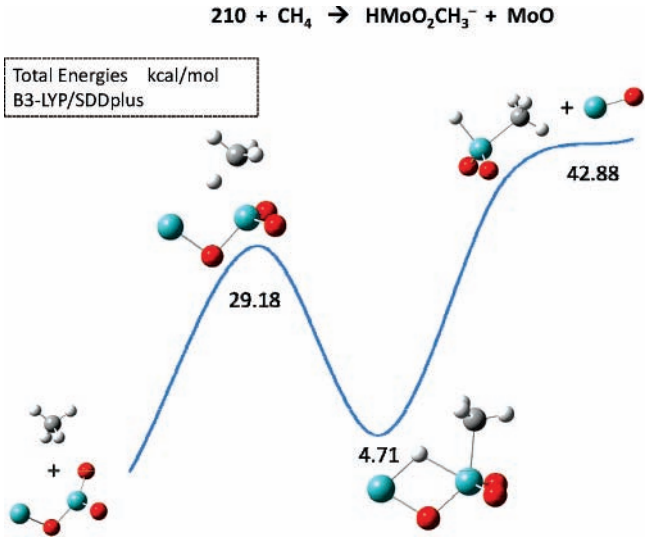

Figure 4. Reaction energy profile for the reaction of the 210 isomer of $Mo_2O_3^-$ with methane.

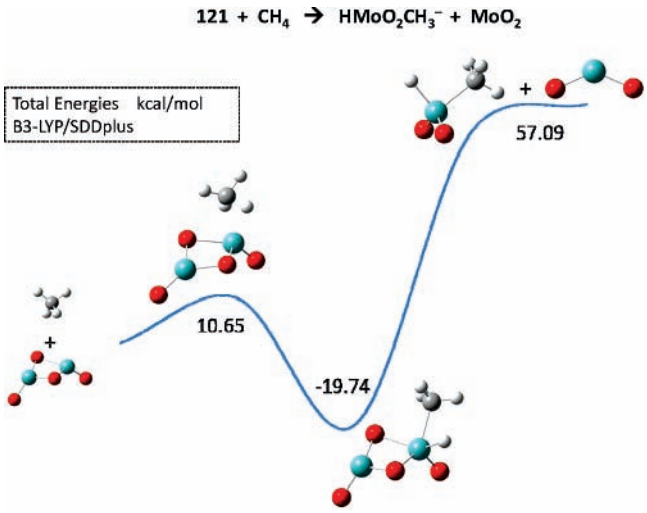

Figure 5. Reaction energy profile for the reaction of the 121 isomer of $Mo_2O_4^-$ with methane.

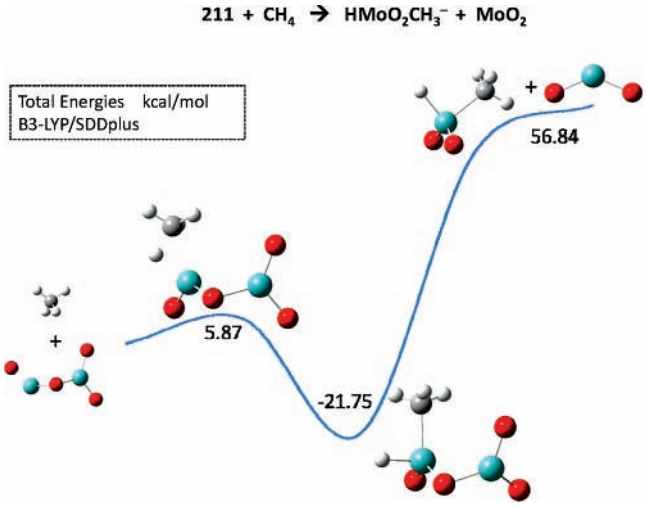

Figure 6. Reaction energy profile for the reaction of the 211 isomer of $Mo_2O_4^-$ with methane.

molecule. This reaction, which is exothermic, would then yield the products listed in Table 3. However, such a mechanism is likely to have an even higher barrier than considered previously because there would be a transition state associated with the insertion of the corresponding neutral product into the second methane's C−H bond. Clearly this is not favorable.

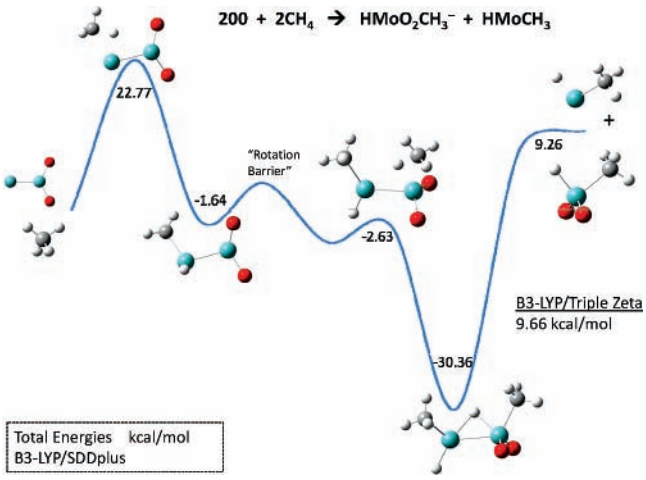

Figure 7. Reaction energy profile for the reaction of the 200 isomer of $Mo_2O_2^-$ with two methanes.

TABLE 3: B3LYP/SDDplus Reaction Energies and Zero-Point Corrected Energies, in kcal/mol, of Reactions of $Mo_2O_n^-$ with Two Methanes Producing Desired Products

		ΔE	ΔE + zpe
$Mo_2O_2^- + 2CH_4 \rightarrow$	$HMoO_2CH_3^- + HMoCH_3$	9.6	3.9
$Mo_2O_3^- + 2CH_4 \rightarrow$	$HMoO_2CH_3^- + HMoOCH_3$	13.0	7.5
$Mo_2O_4^- + 2CH_4 \rightarrow$	$HMoO_2CH_3^- + HMoO_2CH_3$	21.1	17.0
$Mo_2O_5^- + 2CH_4 \rightarrow$	$HMoO_2CH_3^- + HMoO_3CH_3$	37.1	35.5

(2) The $Mo_2O_y^-$ could insert itself into the C−H bond producing the $(CH_4)Mo_2O_y^-$ species as in Figures 2−6. The second molybdenum of this species (the Mo center that has not been inserted into the methane) could then be inserted into the C−H bond of a second methane, producing $(CH_4)_2Mo_2O_y^-$. Having increased the oxidation of both molybdenums, they are now closer to the stoicheometric MoO_3. The fragmentation of this species would then yield the products listed in Table 3. Assuming the barrier for the second methane addition is comparable to the first, mechanism 2 avoids the high barrier associated with the cleavage after adding only one methane.

Although mechanism 2 is a lower energy pathway, it can occur only if the $(CH_4)Mo_2O_y^-$ species exists long enough to react with another methane. Because the first addition of methane is exothermic and performed in the gas phase, in the absence of collisions, the excess energy will be distributed among its 3*n* degrees of freedom. Depending on the experimental conditions, the product may have sufficient energy to fragment. However, because the fragmentation energies are calculated to be quite high and because ion temperatures under the experimental conditions are expected to be moderate, a second reaction with another methane seems feasible.[7]

A thorough search has been performed to find all the possible transition states associated with reactions between $Mo_2O_y^-$ and two methanes. Figures 7−13 show the reaction profiles of the low energy isomers of each $Mo_2O_y^-$ species.

Figure 7 shows methane reacting with the 200 cluster of $Mo_2O_2^-$ at the Mo with the lowest oxidation state. This product, after undergoing a rotation about the Mo−Mo bond, can then exothermically insert the remaining Mo center into the C−H bond of the second methane. This produces a hydrogen bridged species which then can fragment into the experimentally observed products with a ΔE of 9.3 kcal/mol. Although this reaction is thermodynamically feasible, there exists a significant reaction barrier of 22.8 kcal/mol for the first methane addition.

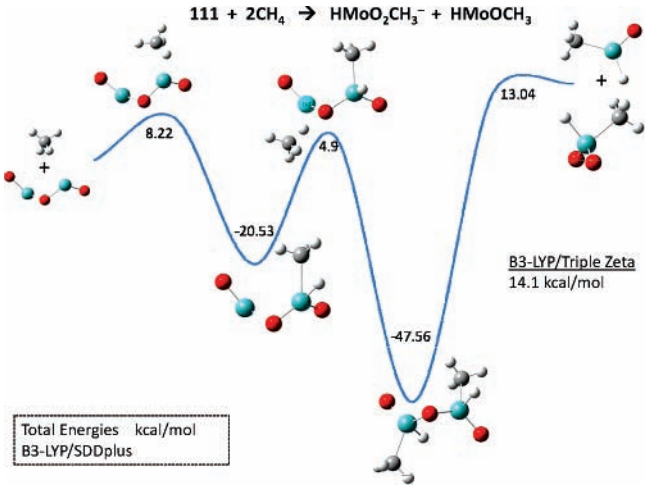

Figure 8. Reaction energy profile for the reaction of the 111 isomer of $Mo_2O_3^-$ with two methanes.

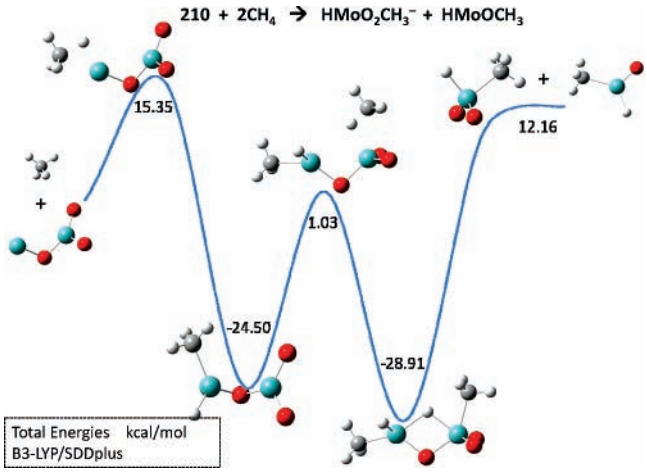

Figure 9. Reaction energy profile for the reaction of the 210 isomer of $Mo_2O_3^-$ with two methanes.

Figure 8 shows methane reacting with the 111 cluster of $Mo_2O_3^-$, which is a slightly more stable isomer (by 0.9 kcal/mol) than 210. Because the 111 cluster belongs to the C_2 symmetry group, addition to either Mo center is equally likely. After the first methane addition (barrier of 8.2 kcal/mol), the second Mo, which is now the lowest oxidation state Mo center, inserts into the C−H bond of the second methane. This produces the $111(CH_4)_2$ product, which after cleavage of a Mo−O bond forms the $HMoO_2CH_3^-$ and a neutral product at a cost of 13.0 kcal/mol.

Figure 9 shows the oxidative addition of methane with the 210 cluster of $Mo_2O_3^-$ at the Mo center with the lowest oxidation state. This initial barrier of 15.4 kcal/mol is nearly twice that of the 111 cluster, demonstrating the importance of proximal electron-withdrawing oxygens. A second C−H bond insertion occurs, producing a species containing both hydrogen and oxygen bridging. This intermediate is now able to form $HMoO_2CH_3^-$ and a neutral product by diagonally cleaving the Mo−O(H)−Mo bridged bond at a final cost of 12.2 kcal/mol.

Figure 10 shows the reaction between methane and the 121 isomer of $Mo_2O_4^-$, which is slightly the more stable than the 211 isomer (0.3 kcal/mol). Although the 121 cluster has only C_s symmetry (the C_{2v} structure is less stable by 0.8 kcal/mol), both of the Mo centers are in very similar chemical environments. Thus, addition to either center should be equally probable. After addition of the first methane, the second methane adds to the second Mo center in much the same fashion as the

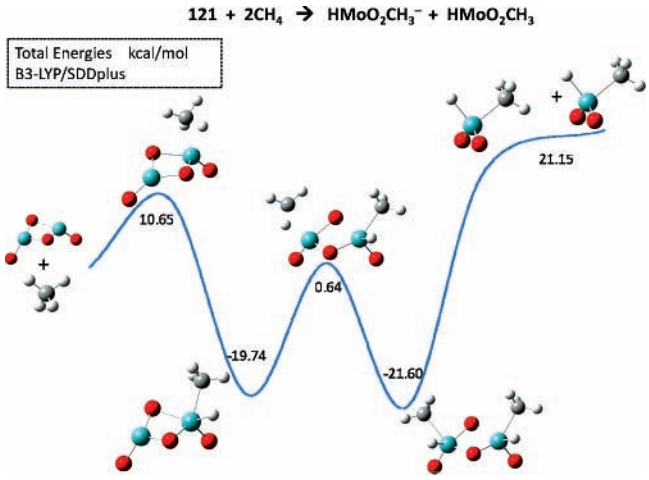

Figure 10. Reaction energy profile for the reaction of the 121 isomer of $Mo_2O_4^-$ with two methanes.

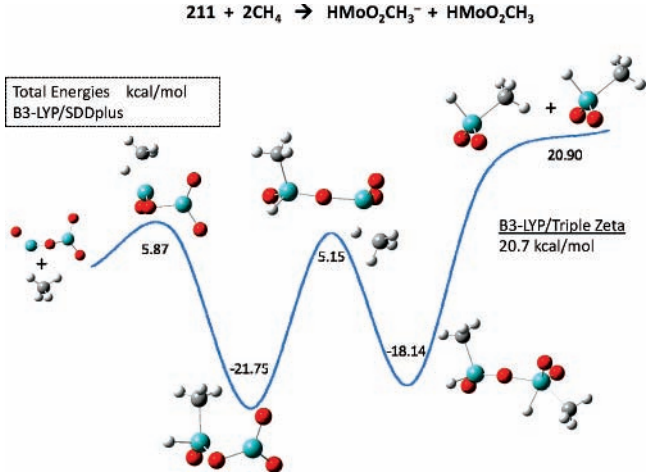

Figure 11. Reaction energy profile for the reaction of the 211 isomer of $Mo_2O_4^-$ with two methanes.

first. The product of both oxidative additions can now form $HMoO_2CH_3^-$ and a neutral product by diagonally cleaving the Mo $-O_2-$Mo bridged bond at a final cost of 21.2 kcal/mol.

Figure 11 shows the reaction between methane and the 211 isomer of $Mo_2O_4^-$. As the lowest oxidation state molybdenum inserts into the first methane, we see the lowest C−H bond insertion barrier (5.8 kcal/mol) for all $Mo_2O_y^-$ clusters. This can be accredited to the fact that, while 211 contains four oxygens that pull electron density away from the molybdenum center, creating a more reactive positive molybdenum, more of the oxygens are closer to the nonreacting Mo. This minimizes steric repulsions between the incoming methane and the negative oxygens. A second methane then reacts with the less reactive metal center to yield a product that, upon cleavage of an Mo−O bond, produces $HMoO_2CH_3^-$ and a neutral molecule of the same formula. This total reaction is endothermic by 20.9 kcal/mol but does not involve an additional barrier.

Figure 12 shows the reaction between methane and the slightly more stable (0.8 kcal/mol) 221 isomer of $Mo_2O_5^-$. Because of the near saturation with oxygens, this cluster has only one reactive Mo with which methane addition is plausible. After the first methane addition, both molybdenum centers are of the +6 oxidation state. Sterically protected by the bound oxygens, the second Mo is unable to react with a methane, shifting the reactive site to the shielding oxygens. In agreement with the work of Goddard and co-workers,[8] we observe a σ-bond metathesis reaction in which the Mo−O bond inserts into the

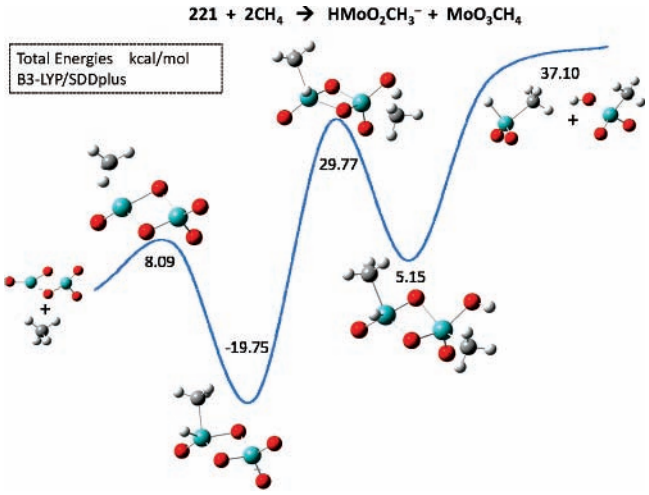

Figure 12. Reaction energy profile for the reaction of the 221 isomer of $Mo_2O_5^-$ with two methanes.

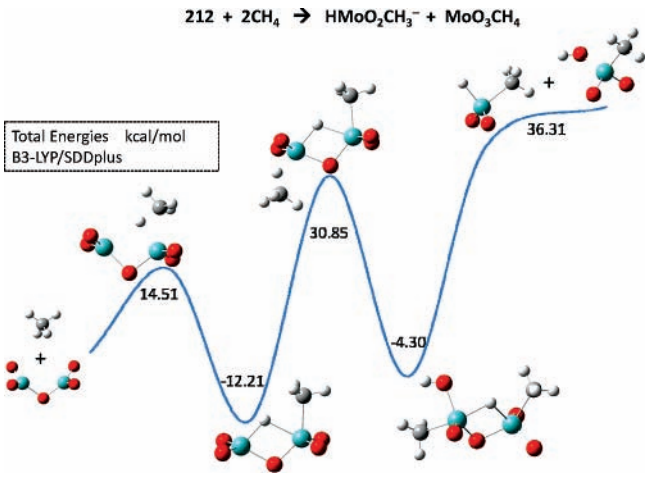

Figure 13. Reaction energy profile for the reaction of the 212 isomer of $Mo_2O_5^-$ with two methanes.

C−H bond. Cleavage of the Mo−O_2−Mo bridged bond then produces $HMoO_2CH_3^-$ and $HMoO_3CH_3$ with a total ΔE_{rxn} of 37.1 kcal/mol.

Figure 13 shows the reaction between methane and the 212 isomer of $Mo_2O_5^-$. Addition to either Mo is equally favorable because 212 belongs to the C_{2v} symmetry point group. As with the other isomer of $Mo_2O_5^-$, addition of the first methane produces a molecule unable to undergo another oxidative addition with methane. To produce the desired products, the (CH_4) 212 species undergoes a σ-bond metathesis reaction much like with 221. Cleavage of this bridged bond yields $HMoO_2CH_3^-$ and $HMoO_3CH_3$ with a total ΔE_{rxn} of 36.3 kcal/mol.

Of all the presently reported reaction profiles, the $Mo_2O_3^-$ (111) + $2CH_4$ reaction produces $HMoO_2CH_3^-$ with the *lowest energy bottleneck*. Although it has neither the lowest insertion barrier (211) nor the lowest endothermicity (200), the experimental appearance of the mass spectrum peak corresponding to $MoO_2CH_4^-$ is likely to be explained by 111 + CH_4 reaction. Furthermore, each mechanism involving two sequential methane insertions is more favorable than the corresponding single methane mechanism. The appeal of this new reaction scheme is seen not only in the dramatic decrease in ΔE_{rxn}(a result of the second methane insertion stabilizing the neutral product) but also in the relative barriers, as the first, and most energetically expensive, methane insertion is able to be performed at

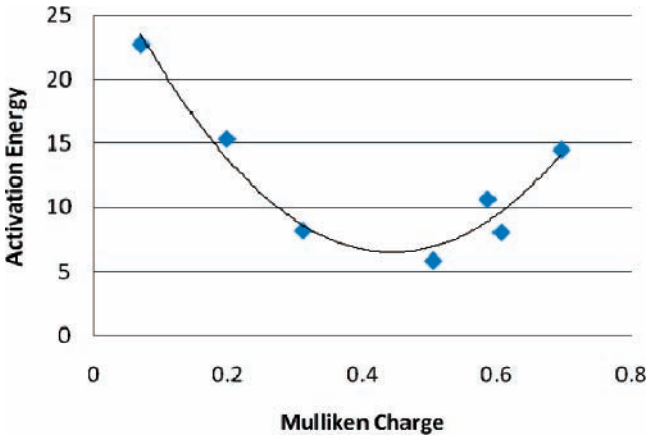

Figure 14. Dependence of the initial insertion barrier on the Mulliken charge on the Mo.

TABLE 4: Mulliken Charge on the Mo Center Which Undergoes the First C−H Bond Insertion for Each Cluster. The Activation Energies are Listed in kcal/mol.

cluster	isomer	charge on Mo	activation energy
$Mo_2O_2^-$	200	0.07	22.77
$Mo_2O_3^-$	210	0.20	15.35
	111	0.31	8.22
$Mo_2O_4^-$	211	0.51	5.87
	121	0.59	10.65
$Mo_2O_5^-$	221	0.61	8.09
	212	0.70	14.51

the most reactive Mo center instead of the center that leads to a product capable of $HMoO_2CH_3^-$ producing cleavage.

The preceding Figures 7−13 show a soft trend in the initial methane insertion barriers. The isomer 200 of $Mo_2O_2^-$ has an initial insertion barrier of 22.8 kcal/mol. As another oxygen is introduced, the 210 and 111 clusters have initial barriers of 15.4 and 8.2 kcal/mol, respectively. For the $Mo_2O_4^-$ isomers, 211 and 121, the first methane adds with respective barriers of only 5.9 and 10.7 kcal/mol. The isomers 221 and 212 have initial barriers of 8.1 and 14.5 kcal/mol, respectively. The trend is such that clusters with more oxygens have lower initial barriers until some maximum number of oxygens is reached, then the barriers start to increase. This can be explained by assuming that the oxidative addition of Mo into methane is kinetically controlled by a balance of the amount of positive charge on the Mo and the magnitude of steric hindrance from bound oxygens. Table 4 below lists each cluster with its Mulliken charge and associated activation energy for the first insertion into methane. This data is then shown graphically in Figure 14.

Figure 14 illustrates the relationship between the Mulliken charge on the reacting metal center and the activation barrier of this reaction. Initial increases in Mulliken charge are accompanied by decreases in activation energy. As the Mulliken charge continues to increase, however, the activation energy begins to increase. Because the increase in positive charge on the Mo is directly related to the number of electronegative oxygens in close proximity, the decrease in activation energy from $Mo_2O_2^-$ to $Mo_2O_3^-$ to $Mo_2O_4^-$ is expected. As the number of oxygens increases to five, the oxygens that were once increasing the reactivity by creating a larger positive charge on Mo are now decreasing the Mo reactivity by sterically shielding the Mo from any methane interaction.

We note that our calculated mechanisms are very different from previously proposed mechanisms for reactions between molybdenum oxides and methane that have oxygen as the active

site.[8,36] These are however usually the reactions of stoicheometric molybdenum oxides (Mo-$_n$O$_{3n}$). Once there are fewer than three oxygens per molybdenum ("suboxide"), it seems as if the active site (whose location depends on a balance between electrostatics and orbital interactions) shifts from the oxygens to the now sterically unhindered molybdenum.

This reaction scheme by which two methanes add sequentially in order to stabilize the neutral fragment as well as the charged ion is likely to be generalized to larger molybdenum suboxides ($Mo_xO_y^-$ with $x \geq 3$ and $y \leq 3x$). Take for example, $Mo_3O_y^-$, by analogy to the $Mo_xO_y^-$ and $Mo_xO_y^-$ series, we should expect the addition of three methanes for a sufficiently oxygen deficient $Mo_3O_y^-$ molecule.

C. Basis Set Dependence of Computed Energies. Table 1 illustrates basis set dependencies in our results for the first four reactions listed in Table 3 in which $Mo_2O_y^-$ reacts with methane to produce $HMoO_2CH_3^-$ and a neutral product. Shown are the differences in reaction energies between the level of theory used thus far (B3LYP/SDDplus) and a larger calibration basis set as discussed earlier (B3LYP/TZ*).[32,33] The difference between the two basis set results is only about 1 kcal/mol. This small variance between reaction energies suggests that our calculations using the augmented "SDDplus" basis set are likely to represent the B3LYP limit.

IV. Conclusions

We have explored all plausible reaction paths for those reactions forming $HMoO_2CH_3^-$ from the $Mo_2O_y^-$ series. Using DFT methods, we have found that: (1) While the reactions between one oxygen and $Mo_xO_y^-$ are highly endothermic and would require conditions of high temperature, the addition of two methanes greatly reduces this thermodynamic cost, making the reactions more physically tractable at lower temperatures. This is a consequence of the second methane insertion stabilizing the neutral product, which is undetectable in experiment. (2) While $Mo_2O_2^-$ and methane is the most thermodynamically favorable reaction, and $Mo_2O_4^-$ with methane is the most kinetically favorable reaction, the $Mo_2O_3^-$ (111 isomer) reaction with methane has the *lowest energy bottleneck* with a barrierless production of $HMoO_2CH_3^-$ that is endothermic by 13.0 kcal/mol (7.5 kcal/mol including zero point energy). (3) The initial insertion of Mo into methane has an activation energy that decreases with the amount of positive charge on the Mo and increases with the magnitude of steric hindrance from bound oxygens. This trend is likely to be generalized to molybdenum suboxide clusters with more than two molybdenums. (4) As an Mo center becomes saturated with oxygens, the active site for reaction with methane shifts from Mo to the bound oxygens, resulting in a σ-bond metathesis reaction in which the Mo—O bond inserts into the C—H bond.

Acknowledgment. The authors would like to acknowledge NSF grant CHE-0616737 at Indiana University for financial support and Prof. Caroline Jarrold and Bruce Yoder for insightful discussions.

Supporting Information Available: The "SDDplus" basis set is obtained by adding the following functions to the SDD basis set for Mo and the D95 basis sets for H, C, and O. This material is available free of charge via the Internet at http://pubs.acs.org.

References and Notes

(1) Borry, R. W.; Kim, Y. H.; Huffsmith, A.; Reimer, J. A.; Iglesia, E. *J. Phys. Chem. B* **1999**, *103*, 5787−5796.

(2) Liu, S. T.; Wang, L.; Ohnishi, R.; Ichikawa, M. *J. Catal.* **1999**, *181*, 175−188.

(3) Ohnishi, R.; Liu, S. T.; Dong, Q.; Wang, L.; Ichikawa, M. *J. Catal.* **1999**, *182*, 92−103.

(4) Shu, J.; Adnot, A.; Grandjean, B. P. A. *Ind. Eng. Chem. Res.* **1999**, *38*, 3860−3867.

(5) Wang, D. J.; Lunsford, J. H.; Rosynek, M. P. *J. Catal.* **1997**, *169*, 347−358.

(6) Zhou, T. J.; Liu, A. M.; Mo, Y. R.; Zhang, H. B. *J. Phys. Chem. A* **2000**, *104*, 4505−4513.

(7) Wyrwas, R. B.; Yoder, B. L.; Maze, J. T.; Jarrold, C. C. *J. Phys. Chem. A* **2006**, *110*, 2157−2164.

(8) Xu, X.; Faglioni, F.; Goddard, W. A. *J. Phys. Chem. A* **2002**, *106*, 7171−7176.

(9) Armentrout, P. B. *J. Phys. Chem. A* **2006**, *110*, 8327−8338.

(10) Bell, R. C.; Castleman, A. W. *J. Phys. Chem. A* **2002**, *106*, 9893−9899.

(11) Cotton, F. A. *J.Chem. Soc., Dalton Trans.* **2000**, 1961−1968.

(12) Hwang, D. Y.; Mebel, A. M. *J. Phys. Chem. A* **2002**, *106*, 12072−12083.

(13) Labinger, J. A.; Bercaw, J. E. *Nature* **2002**, *417*, 507−514.

(14) Matsuoka, Y.; Niwa, M.; Murakami, Y. *J. Phys. Chem.* **1990**, *94*, 1477−1482.

(15) Oyama, S. T.; Radhakrishnan, R.; Seman, M.; Kondo, J. N.; Domen, K.; Asakura, K. *J. Phys. Chem. B* **2003**, *107*, 1845−1852.

(16) Palmer, M. S.; Neurock, M.; Olken, M. M. *J. Am. Chem. Soc.* **2002**, *124*, 8452−8461.

(17) Zhai, H. J.; Wang, L. S. *J. Chem. Phys.* **2006**, *125*, 9.

(18) Bondarchuk, O.; Huang, X.; Kim, J.; Kay, B. D.; Wang, L. S.; White, J. M.; Dohnalek, Z. *Angew. Chem., Int. Ed.* **2006**, *45*, 4786−4789.

(19) Li, S. G.; Dixon, D. A. *J. Phys. Chem. A* **2006**, *110*, 6231−6244.

(20) Huang, X.; Zhai, H. J.; Waters, T.; Li, J.; Wang, L. S. *Angew. Chem., Int. Ed.* **2006**, *45*, 657−660.

(21) Huang, X.; Zhai, H. J.; Li, J.; Wang, L. S. *J. Phys. Chem. A* **2006**, *110*, 85−92.

(22) Zhai, H. J.; Huang, X.; Waters, T.; Wang, X. B.; O'Hair, R. A. J.; Wedd, A. G.; Wang, L. S. *J. Phys. Chem. A* **2005**, *109*, 10512−10520.

(23) Zhai, H. J.; Huang, X.; Cui, L. F.; Li, X.; Li, J.; Wang, L. S. *J. Phys. Chem. A* **2005**, *109*, 6019−6030.

(24) Sun, Q.; Rao, B. K.; Jena, P.; Stolcic, D.; Kim, Y. D.; Gantefor, G.; Castleman, A. W. *J. Chem. Phys.* **2004**, *121*, 9417−9422.

(25) Becke, A. D. *J. Chem. Phys.* **1993**, *98*, 5648−5652.

(26) Lee, C. T.; Yang, W. T.; Parr, R. G. *Phys. Rev. B* **1988**, *37*, 785−789.

(27) Bergner, A.; Dolg, M.; Kuchle, W.; Stoll, H.; Preuss, H. *Mol. Phys.* **1993**, *80*, 1431−1441.

(28) Dolg, M.; Stoll, H.; Preuss, H.; Pitzer, R. M. *J. Phys. Chem.* **1993**, *97*, 5852−5859.

(29) Dolg, M.; Wedig, U.; Stoll, H.; Preuss, H. *J. Chem. Phys.* **1987**, *86*, 866−872.

(30) Jensen, F. *Introduction to Computational Chemistry*, 2nd ed.; John Wiley & Sons: Chichester, U.K., 2007.

(31) Dunning, T. H. *J. Chem. Phys.* **1970**, *53*, 2823-&.

(32) Martin, J. M. L.; Sundermann, A. *J. Chem. Phys.* **2001**, *114*, 3408−3420.

(33) Dunning, T. H. *J. Chem. Phys.* **1989**, *90*, 1007−1023.

(34) Frisch, M. J.; Trucks, G. W.; Schlegel, H. B.; Scuseria, G. E.; Robb, M. A.; Cheeseman, J. R.; Montgomery, J. A., Jr.; Vreven, T.; Kudin, K. N.; Burant, J. C.; Millam, J. M.; Iyengar, S. S.; Tomasi, J.; Barone, V.; Mennucci, B.; Cossi, M.; Scalmani, G.; Rega, N.; Petersson, G. A.; Nakatsuji, H.; Hada, M.; Ehara, M.; Toyota, K.; Fukuda, R.; Hasegawa, J.; Ishida, M.; Nakajima, T.; Honda, Y.; Kitao, O.; Nakai, H.; Klene, M.; Li, X.; Knox, J. E.; Hratchian, H. P.; Cross, J. B.; Bakken, V.; Adamo, C.; Jaramillo, J.; Gomperts, R.; Stratmann, R. E.; Yazyev, O.; Austin, A. J.; Cammi, R.; Pomelli, C.; Ochterski, J. W.; Ayala, P. Y.; Morokuma, K.; Voth, G. A.; Salvador, P.; Dannenberg, J. J.; Zakrzewski, V. G.; Dapprich, S.; Daniels, A. D.; Strain, M. C.; Farkas, O.; Malick, D. K.; Rabuck, A. D.; Raghavachari, K.; Foresman, J. B.; Ortiz, J. V.; Cui, Q.; Baboul, A. G.; Clifford, S.; Cioslowski, J.; Stefanov, B. B.; Liu, G.; Liashenko, A.; Piskorz, P.; Komaromi, I.; Martin, R. L.; Fox, D. J.; Keith, T.; Al-Laham, M. A.; Peng, C. Y.; Nanayakkara, A.; Challacombe, M.; Gill, P. M. W.; Johnson, B.; Chen, W.; Wong, M. W.; Gonzalez, C.; Pople, J. A. *Gaussian 03*, revision E.X2; Gaussian, Inc.: Wallingford, CT, 2004.

(35) Yoder, B. L.; Maze, J. T.; Raghavachari, K.; Jarrold, C. C. *J. Chem. Phys.* **2005**, *122*, 094313.

(36) Fu, G.; Xu, X.; Lu, X.; Wan, H. L. *J. Am. Chem. Soc.* **2005**, *127*, 3989−3996.